Accessing the pion distribution amplitude through the CLEO and E791 data

Alexander P. Bakulev[1], **S. V. Mikhailov**[2]

Joint Institute for Nuclear Research, Bogoliubov Lab. of Theoretical Physics, 141920, Moscow Region, Dubna, Russia

N. G. Stefanis[3]

Institut für Theoretische Physik II, Ruhr-Universität Bochum, I-44780 Bochum, Germany

Abstract

Using QCD perturbation theory in NLO and light-cone QCD sum rules, we extract from the CLEO experimental data on the $F^{\gamma^*\gamma\pi}\left(Q^2\right)$ transition form factor constraints on the Gegenbauer coefficients a_2 and a_4, as well as on the inverse moment $\langle x^{-1}\rangle_\pi$ of the pion distribution amplitude. We show that both the asymptotic and the Chernyak–Zhitnitsky pion distribution amplitudes are excluded at the 3σ- and 4σ-level, respectively, while the data confirms the end-point suppressed shape of the pion DA we previously obtained with QCD sum rules and nonlocal condensates. These findings are also supported by the data of the Fermilab E791 experiment on diffractive dijet production.

PACS: 11.10.Hi,12.38.Bx,12.38.Lg,13.40.Gp

Keywords: Transition form factor, Pion distribution amplitude, QCD sum rules, Factorization, Renormalization group evolution

1 Introduction

Perturbative QCD describes the short-distance interactions of quarks and gluons and can be applied to the description of hadronic reactions on account of factorization theorems. More precisely, one can calculate systematically perturbative kernels and associated anomalous dimensions that govern the evolution of hadron distribution amplitudes (DAs). These DAs parameterize hadronic matrix elements of quark-gluon currents and have to be determined by nonperturbative methods or extracted from experimental data. Recently, Schmedding and Yakovlev [1] have presented an analysis, based on light-cone QCD sum rules (LCSR) proposed earlier by Khodjamirian [2] and taking into account $O(\alpha_s)$-corrections, of the high-precision CLEO experimental data [3] that allows to extract quite restrictive constraints on the first two Gegenbauer coefficients a_2 and a_4 which control the x-dependence of the pion distribution amplitude (πDA). This sort of analysis was further extended and refined by us in [4, 5] with the aim to take more properly into account NLO

[1]E-mail: bakulev@thsun1.jinr.ru
[2]E-mail: mikhs@thsun1.jinr.ru
[3]E-mail: stefanis@tp2.ruhr-uni-bochum.de

evolution effects of the πDA, to treat threshold effects of the effective strong coupling, and to estimate more carefully contributions resulting from (unknown) higher-twist effects. In addition, we derived directly from the CLEO data estimates for the inverse moment of the πDA, which is compatible with that obtained from an *independent* QCD sum rule, referring in both cases to the same low-momentum scale of the order of 1 GeV^2.

The results of our analysis, presented here, lead to the conclusion that the Chernyak–Zhitnitsky model [6] for the πDA in the plane (a_2, a_4) is outside the 4σ-level, while the asymptotic DA, is excluded at the 3σ level. In fact, the data seem to prefer end-point-suppressed DAs as those we have previously determined using QCD sum rules with non-local condensates [4]. These conclusions are further supported by contrasting the above mentioned πDAs with the E791 dijet data [7] following the convolution approach of Braun et al. [8]. Moreover, it was found [5] that the CLEO data are sensitive to the value of the average vacuum quark virtuality, limiting its value close to $\lambda_q^2 = 0.4$ GeV^2.

2 What is the pion distribution amplitude $\varphi_\pi(x, \mu^2)$?

The πDA is a central object in the deeper understanding of the pion microscopic structure in terms of quark and gluon degrees of freedom within QCD. This amplitude is defined by the matrix element of a nonlocal axial current on the light cone:

$$\langle 0|\bar{d}(z)\gamma_\mu\gamma_5 E(z,0)u(0)|\pi(P)\rangle\Big|_{z^2=0} \;=\; if_\pi P_\mu \int_0^1 dx\; e^{ix(zP)}\;\varphi_\pi^{\text{Tw-2}}(x,\mu^2)\,, \qquad (1)$$

where gauge-invariance is ensured due to the Fock–Schwinger string $E(z,0) = \mathcal{P}e^{ig\int_0^z A_\mu(\tau)d\tau^\mu}$ and $\varphi_\pi^{\text{Tw-2}}(x,\mu^2)$ is symmetric with respect to $x \leftrightarrow \bar{x}$ ($\bar{x} \equiv 1-x$) and is normalized to unity, whereas μ^2 denotes the normalization scale. Fig. 1 visualizes the light-cone structure of the πDA. There are also 6 pion DAs at twist-4 level, four of them contributing to

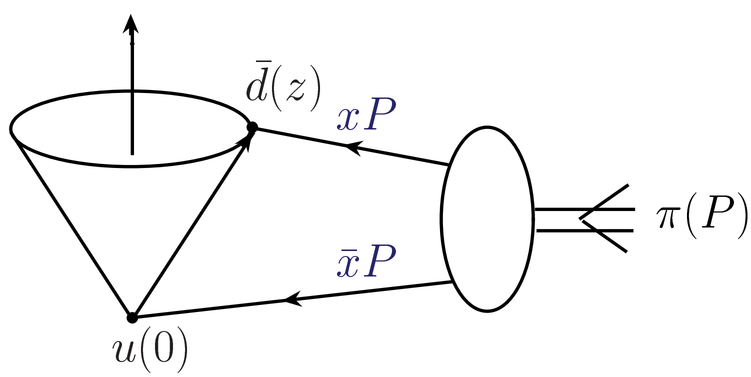

Figure 1: $\varphi_\pi(x;\mu^2)$ – light-cone amplitude for the transition $\pi \to u + d$.

the $\gamma^*\gamma \to \pi$-transition as a twist-4 correction, whose value is parameterized by the scale $\delta^2_{\text{Tw-4}} \approx 0.19$ GeV^2. In what follows we will speak mainly of the twist-2 πDA and for the sake of brevity we will omit its superscript $^{\text{Tw-2}}$ referring to it simply as $\varphi_\pi(x;\mu^2)$.

Due to vector current conservation, the solution of the ERBL evolution equation [9, 10] (in LO approximation) in the asymptotic limit is $\varphi_\pi(x;\mu^2 \to \infty) = \varphi^{\text{As}}(x) = 6x(1-x)$. A particularly convenient way to represent the πDA is to use its 1-loop eigenfunctions, viz.,

the Gegenbauer polynomials [9]:

$$\varphi_\pi(x;\mu^2) = \varphi^{\rm As}(x)\Big[1 + a_2(\mu^2)C_2^{3/2}(\xi) + a_4(\mu^2)C_4^{3/2}(\xi) + ...\Big]_{\xi\equiv 2x-1} \tag{2}$$

with $C_n^{3/2}(\xi)$ being the Gegenbauer polynomials and the ellipsis denoting still higher-order eigenfunctions than displayed. In this representation all the dependence of $\varphi_\pi(x;\mu^2)$ on μ^2 is concentrated in the coefficients $a_n(\mu^2)$ due to the fact that the 1-loop evolution kernel has a factorized structure $V_{\text{1-loop}}(x,x';\alpha_s) = [\alpha_s/(4\pi)]V_0(x,x')$. In the NLO approximation the eigenfunctions of the evolution kernel inevitably depend on α_s and therefore on μ^2. Note that because of the symmetry in $x \leftrightarrow \bar{x}$, only even Gegenbauer polynomials contribute.

The high precision of the CLEO data provides the possibility to extract these important theoretical parameters (a_2 and a_4) directly from experiment. But before we turn to this subject, let us first give some brief exposition of the theoretical method to determine the πDA within the QCD sum-rule approach.

3 QCD sum rules with nonlocal condensates

To model the nonlocality of the QCD vacuum, we assume $\langle\bar{q}(0)q(z)\rangle = \langle\bar{q}(0)q(0)\rangle e^{-|z^2|\lambda_q^2/8}$, and similar expressions for other nonlocal condensates (NLCs), where a single scale parameter $\lambda_q^2 = \langle k^2\rangle$ was introduced in order to characterize the average momentum of quarks in the QCD vacuum [11]:

$$\lambda_q^2 = \begin{cases} 0.4 \pm 0.1\ \text{GeV}^2 & \text{from QCD SRs [12];} \\ 0.5 \pm 0.05\ \text{GeV}^2 & \text{from QCD SRs [13];} \\ \approx 0.4 - 0.5\ \text{GeV}^2 & \text{from lattice QCD [14, 15].} \end{cases}$$

The correlation length $\lambda_q^{-1} \simeq 0.3$ Fm $\sim$ ρ-meson size represents the width of the NLC at small distances. Let us mention that for very large distances ($z \gg 1$ Fm [15]) one may assume another form of the condensate, given by [16] $\langle\bar{q}(0)q(z)\rangle \sim \langle\bar{q}(0)q(0)\rangle e^{-|z|\Lambda}$ at $|z| \gg 1$ Fm (with $\Lambda \simeq 450$ MeV). This behavior is of no importance in the problem under investigation.

In [4] we have determined all coefficients up to order $n = 10$ using QCD sum rules with nonlocal condensates. It turned out that all coefficients beyond $n = 4$ are very small so that for practical purposes it suffices to model the πDA using only a_2 and a_4. So, the NLC QCD sum rules produces a whole bunch of self-consistent 2-parameter model DAs (see Fig. 2a.) at $\mu^2 \simeq 1$ GeV^2:

$$\varphi_\pi(x) = \varphi^{\rm as}(x)\left[1 + a_2 C_2^{3/2}(2x-1) + a_4 C_4^{3/2}(2x-1)\right] \tag{3}$$

with the best-fit model (bold-faced on Fig. 2a) defined by the parameters

$$a_2^{\textbf{b.f.}} \;=\; +0.188\,; \qquad a_4^{\textbf{b.f.}} \;=\; -0.130\,. \tag{4}$$

The admissible regions for the parameters a_2, a_4 of the πDA are presented in Fig. 2b as shaded slanted rectangles and are shown for different values of λ_q^2. Fig. 2a demonstrates the most striking feature of our type of πDAs: their end-points (i. e., $x \to 0$ and $x \to 1$) are strongly suppressed, the suppression being controlled by the quark vacuum virtuality λ_q^2. Both the asymptotic and the CZ πDAs are *not* end-point suppressed, as we have quantitatively shown in [4]. Our models demonstrate by a precedent that the common statement *"two-humped πDAs are end-point concentrated"* is wrong.

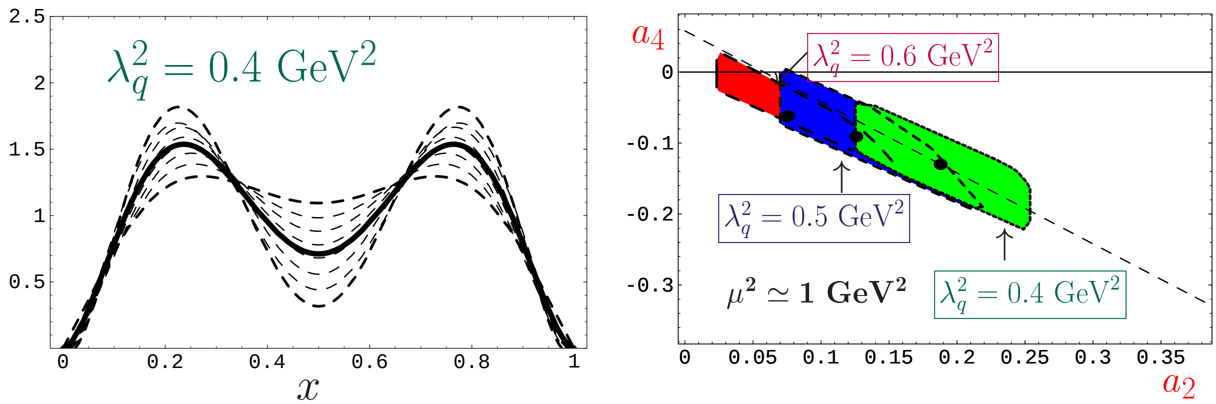

Figure 2: **Left (a):** Self-consistent 2-parameter bunch of admissible πDAs. **Right (b):** Admissible regions for the parameters a_2 and a_4 of the πDA.

4 $\gamma^*\gamma \to \pi$: Why Light-Cone Sum Rules?

For $Q^2 \gg m_\rho^2$, $q^2 \ll m_\rho^2$, pQCD factorization does not help because it is valid only for leading twist and therefore higher twists become important [17]. The reason for this

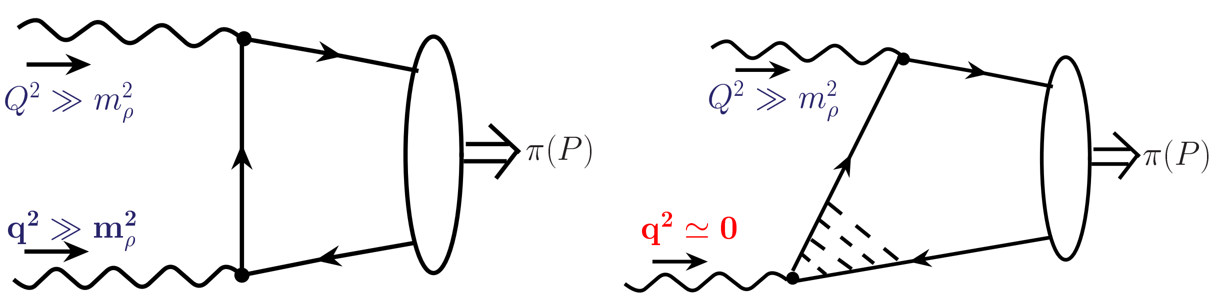

Figure 3: Left part demonstrates the regime when pQCD description is valid; right part makes explicit why LCSR should be applied.

failure can be understood by recalling that if $q^2 \to 0$, one needs to take into account the interaction of a real photon at long distances of the order of $O(1/\sqrt{q^2})$, as the following Fig. 3 illustrates. To account for long-distance effects in a perturbative QCD treatment, one needs to introduce the light-cone DA of a real photon.

To this end, Khodjamirian [2] has shown that light-cone QCD sum rules (LCSR) effectively account for the long-distance effects of a real photon by using quark-hadron duality in the vector channel and an appropriate dispersion relation in q^2; namely,

$$F_{\gamma\gamma^*\pi}(Q^2, q^2) = \frac{1}{\pi}\int_0^{s_0} \frac{\rho(Q^2, s)}{m_\rho^2 + q^2} \exp\left[\frac{m_\rho^2 - s}{M^2}\right] ds + \frac{1}{\pi}\int_{s_0}^{\infty} \frac{\rho(Q^2, s)}{s + q^2} ds\,, \qquad (5)$$

where $s_0 \simeq 1.5$ GeV^2 is an effective threshold in the vector channel and the Borel parameter M^2 takes values in the range $0.5 - 0.9$ GeV^2. Then, the real photon limit ($q^2 \to 0$) becomes

safely accessible. Here $\rho(Q^2, s) = \mathbf{Im} F^{\rm PT}_{\gamma^*\gamma^*\pi}(Q^2, -s)$ includes contributions from both the leading twist πDA as well as the twist-4 one. The latter is characterized by the twist-4 scale parameter $\delta^2_{\text{Tw-4}}$. This theoretical ground was extended by Schmedding&Yakovlev (SY) to the NLO accuracy [1].

5 Results from nonlocal QCD sum rules vs CLEO constraints

In [5] we improved the SY analysis based on LCSR (5) by taking into account ERBL NLO evolution for the πDA and the exact NLO running of $\alpha_s(Q^2)$. The established relation $\delta^2_{\text{Tw-4}} \approx \lambda_q^2/2$ has been also involved in the analysis. As Fig. 4a shows, we obtained reasonable agreement with established in this approach constraints just for the value of $\lambda_q^2 = 0.4$ GeV^2.

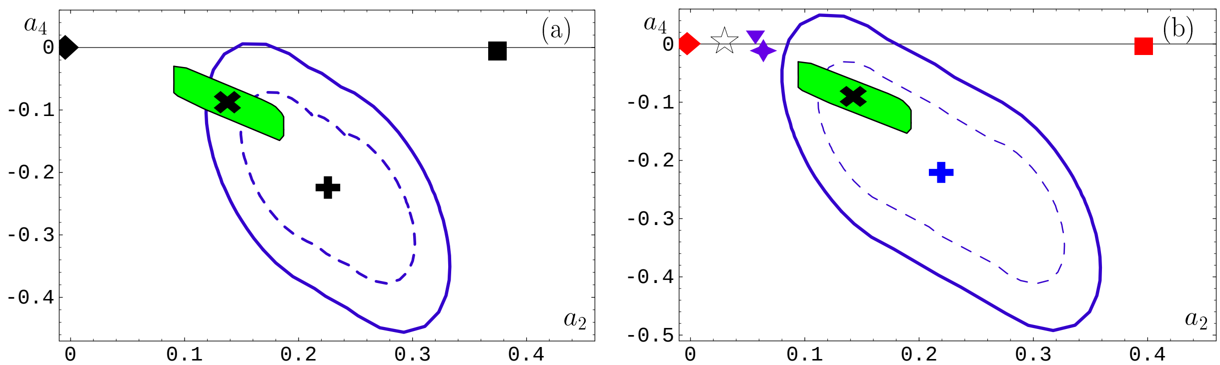

Figure 4: Comparison of theoretical predictions of nonlocal QCD sum rules for $\lambda_q^2 =$ 0.4 GeV^2 and the CLEO data constraints obtained in the LCSR approach. **Left (a):** Previous [5] results. **Right (b):** New BMS [18] constraints. Here: ◆ = asymptotic DA, ✖ = BMS model, ■ = CZ DA, ✚ = best-fit point, ☆ [19] and ✥ [20] = instanton models, ▼ = transverse lattice result [21]. All values are evaluated at $\mu^2_{\text{SY}} = (2.4\text{ GeV})^2$.

More recently [18], we have refined this extensive analysis in several respects, notably, by obtaining from the CLEO data direct estimate for the inverse moment of the πDA that plays a crucial role in pion electromagnetic/transition form factors and by verifying the reliability of the main results of the CLEO data analysis quantitatively. We also refined our error analysis by taking into account the total uncertainty of the twist-4 contribution and treated the threshold effects in the strong running coupling more accurately. The main upshot of this investigation is presented graphically in Fig. 4b, where the values $\lambda_q^2 = 0.4$ GeV^2 and $\delta^2_{\text{Tw-4}} = 0.19(4)$ GeV^2 have been employed. One can see that even with a 20% uncertainty in the twist-4 contribution, the CZ distribution amplitude (■) is excluded – at least – at the 4σ-level, while other well-known models (☆, ✥ and ▼) with shapes more or less close to the asymptotic one (◆) are excluded at the 2σ-level.

These findings are further supported by extracting the inverse moment of the πDA from the CLEO data in a two-Gegenbauer model, $a_2 + a_4 = \langle x^{-1}\rangle^{\exp}_\pi(\mu_0^2)/3 - 1$, at the low scale $\mu_0^2 = 1$ GeV^2. The obtained constraints are presented in Fig. 5b. One should compare them with the theoretical model-independent estimate of the inverse moment $\langle x^{-1}\rangle^{\rm SR}_\pi(\mu_0^2 \approx 1\text{ GeV}^2) = 3.28 \pm 0.31$, obtained in the special NLC QCD sum rule using

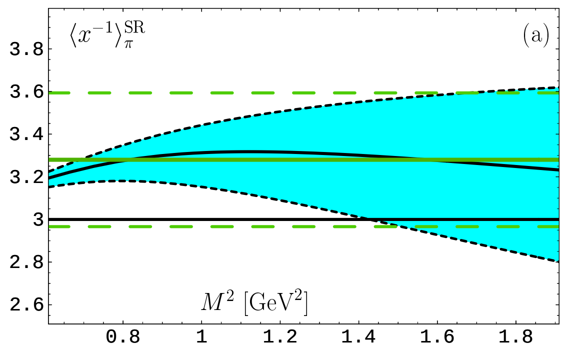

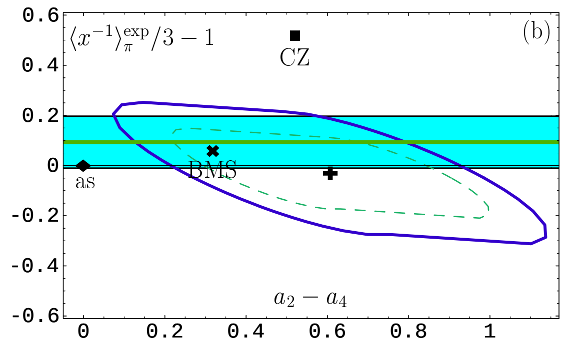

Figure 5: **Left (a):** The inverse moment $\langle x^{-1}\rangle_\pi^{\rm SR}$ shown as a function of the Borel parameter M^2 from the special NLC QCD sum rule at the scale μ_0^2 [4]; the light solid line is the estimate for $\langle x^{-1}\rangle_\pi^{\rm SR}$; the dashed lines correspond to its error-bars. **Right (b):** The result of the CLEO data processing for the quantity $\langle x^{-1}\rangle_\pi^{\rm exp}/3-1$ at the scale $\mu_0^2 \approx 1$ GeV^2 in comparison with three theoretical models from QCD sum rules, CZ, BMS, and (a). The thick solid-line contour corresponds to the union of 2σ-contours, while the thin dashed-line contour denotes the union of 1σ-contours. The light solid line with the hatched band indicates the mean value of $\langle x^{-1}\rangle_\pi^{\rm SR}/3-1$ and its error bars in part (a).

again $\lambda_q^2 = 0.4$ GeV^2 [22, 4], see Fig. 5a. Noteworthily, these constraints match each other and both of them comply with the value $\frac{1}{3}\langle x^{-1}\rangle_\pi - 1 = 0.24 \pm 0.16$ found in [23] from a LCSR analysis of electromagnetic pion form factor. From Fig. 5b it is evident that again both the asymptotic πDA and the CZ model are far outside the region of the CLEO experimental data.

6 E791: Diffractive dijet production

The Fermilab group E791 proposed [7] to exploit experimentally the ideas on dijet diffractive dissociation suggested in [24] and further developed in [25, 26, 8]. Braun et al. [8] have used a convolution-type approach to account for hard-gluon exchanges, represented diagrammatically in the left part of Fig. 6. Following this convolution procedure (having also recourse to [27]), and ignoring the distortion of our predictions caused by the detector acceptance, we found the results displayed in the right part of Fig. 6, making evident that, though the data from E791 are not that sensitive as to exclude other shapes for the pion DA (asymptotic and CZ model), also displayed for the sake of comparison, they are relatively in good agreement with our predictions. Especially, in the middle x region, where our πDAs – the shaded strip – has the largest uncertainties (see Fig. 2a), the predictions are not in conflict with the data. However, before this data set can be used for a quantitative comparison, its inherent uncertainties have to be removed.

It is again worth emphasizing that because our model distribution amplitudes – exemplified by the BMS model – are end-point suppressed (see Fig. 7), they are not affected by the poor accuracy of the E791 experimental data in these regions.

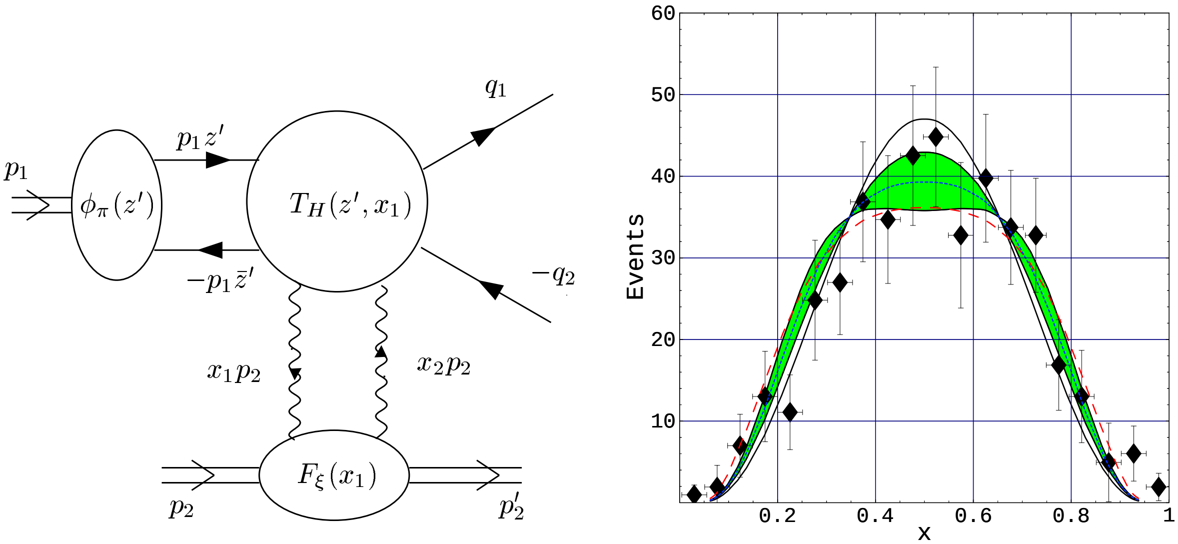

Figure 6: **Left:** Diffractive dijet πA-production in the E791 experiment with $q_\perp^2 \simeq 4$ GeV^2 and $s \simeq 1000$ GeV^2. **Right:** Asymptotic DA (solid line), CZ DA (dashed line) and BMS bunch (shaded strip) in comparison with E791 data. Corresponding χ^2 are: 12.56, 14.15 and 10.96 (the last for BMS model with $\lambda_q^2 = 0.4$ GeV^2).

7 Conclusions

Thanks to the recent high-precision CLEO experimental data [3], we can answer more questions of nonperturbative QCD than a couple of years before. On the theoretical side, the method of QCD sum rules with nonlocal condensates [11, 22, 15, 4] provided a tool to determine more precisely than before a bunch of candidate DAs for the pion that are endpoint-suppressed due to a rather large QCD vacuum quark virtuality λ_q^2. On the other hand, the method of light-cone sum rules [2, 1, 5] enables us to access the pion-photon transition form factor when one photon becomes real. Taking these theoretical approaches in conjunction, we were able to analyze the CLEO data at the NLO level in order to derive restrictive constraints on the first two Gegenbauer coefficients a_2 and a_4, which control the x-dependence of the πDA. These parameters allow the reconstruction of the πDA and

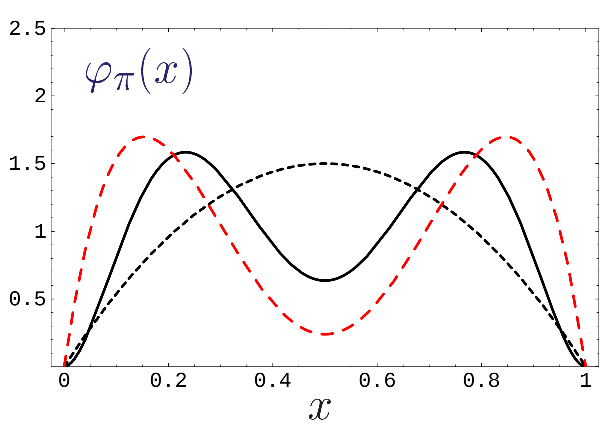

Figure 7: Comparison of different DA curves aiming to illustrate the end-point suppression of the BMS model: CZ (dashed), asymptotic (dotted) and BMS (solid).

can be further tested against other experimental data, like those collected in the dijet production Fermilab experiment E791. The main conclusion is that both the CZ model as well as the asymptotic πDA are excluded—at least at the 2σ level—by the CLEO data, while the two-humped end-point suppressed BMS distribution amplitude with a value of $\lambda_q^2 \approx 0.4$ GeV^2 is in a good agreement with the CLEO data and not in contradiction with the E791 data.

Acknowledgments
One of us (A.P.B.) would like to thank the organizers of the Conference NAPP-2003 for the invitation and support. This work was supported in part by INTAS-CALL 2000 N 587, the RFBR (grant 03-03-16816), the Heisenberg–Landau Programme (grants 2002 and 2003), the COSY Forschungsprojekt Jülich/Bochum, and the Deutsche Forschungsgemeinschaft.

References

[1] A. Schmedding and O. Yakovlev, Phys. Rev. D 62 (2000) 116002.

[2] A. Khodjamirian, Eur. Phys. J. C 6 (1999) 477.

[3] J. Gronberg et al., CLEO Collaboration, Phys. Rev. D 57 (1998) 33.

[4] A. P. Bakulev, S. V. Mikhailov, and N. G. Stefanis, Phys. Lett. B 508 (2001) 279; in: Proceedings of the 36th Rencontres de Moriond on QCD and Hadronic Interactions, 17-24 March 2001, Les Arcs, France, pp. 133-136 [arXiv:hep-ph/0104290].

[5] A. P. Bakulev, S. V. Mikhailov, and N. G. Stefanis, Phys. Rev. D 67 (2003) 074012.

[6] V. L. Chernyak and A. R. Zhitnitsky, Phys. Rep. 112 (1984) 173.

[7] E. M. Aitala et al., Fermilab E791 Collaboration, Phys. Rev. Lett. 86 (2001) 4768.

[8] V. M. Braun et al., Nucl. Phys. B 638 (2002) 111.

[9] A. V. Efremov and A. V. Radyushkin, Phys. Lett. B 94 (1980) 245; Theor. Math. Phys. 42 (1980) 97.

[10] G. P. Lepage and S. J. Brodsky, Phys. Lett. B 87 (1979) 359; Phys. Rev. D 22 (1980) 2157.

[11] S. V. Mikhailov and A. V. Radyushkin, Sov. J. Nucl. Phys. 49 (1989) 494; Phys. Rev. D 45 (1992) 1754.

[12] V. M. Belyaev and B. L. Ioffe, Sov. Phys. JETP 57 (1983) 716;
A. A. Ovchinnikov and A. A. Pivovarov, Sov. J. Nucl. Phys. 48 (1988) 721.

[13] A. A. Pivovarov, Bull. Lebedev Phys. Inst. 5 (1991) 1.

[14] M. D'Elia, A. Di Giacomo, and E. Meggiolaro, Phys. Rev. D59 (1999) 054503.

[15] A. P. Bakulev and S. V. Mikhailov, Phys. Rev. D 65 (2002) 114511.

[16] A. P. Bakulev and S. V. Mikhailov, Z. Phys. C 68 (1995) 451.

[17] A. V. Radyushkin and R. Ruskov, Nucl. Phys. B 481 (1996) 625.

[18] A. P. Bakulev, S. V. Mikhailov, and N. G. Stefanis, [arXiv: hep-ph/0303039].

[19] V. Y. Petrov et al., Phys. Rev. D 59 (1999) 114018.

[20] M. Praszalowicz and A. Rostworowski, Phys. Rev. D 64 (2001) 074003.

[21] S. Dalley and B. van de Sande, Phys. Rev. D 67 (2003) 114507.

[22] A. P. Bakulev and S. V. Mikhailov, Phys. Lett. B 436 (1998) 351.

[23] J. Bijnens, A. Khodjamirian, Eur. Phys. J. C 26 (2002) 67.

[24] L. Frankfurt, G. A. Miller, and M. Strikman, Phys. Lett. B 304 (1993) 1.

[25] N. N. Nikolaev, W. Schäfer, and G. Schwiete, Phys. Rev. D 63 (2001) 014020.

[26] V. Chernyak, Phys. Lett. B 516 (2001) 116; V. L. Chernyak and A. G. Grozin, Phys. Lett. B 517 (2001) 119.

[27] A. Freund and M. F. McDermott, Phys. Rev. D 65 (2002) 074008; A. D. Martin, R. G. Roberts, and W. J. Stirling, Phys. Lett. B 354 (1995) 155.